IUST
Iran University of Science and Technology

Iranian Journal of Electrical and Electronic Engineering

Journal Homepage: ijeee.iust.ac.ir

Research Paper

A Novel Droop-based Control Strategy for Improving the Performance of VSC-MTDC Systems in Post-Contingency Conditions

S. M. Alavi* and R. Ghazi*(C.A.)

Abstract: One of the significant concerns in the MTDC systems is that voltage source converters (VSCs) do not hit their limits in the post-contingency conditions. Converters outage, DC line disconnection, and changeable output power of wind farms are the most common threats in these systems. Therefore, their destructive impact on neighboring AC systems should be minimized as much as possible. The fixed droop control is a better choice than others to deal with this, although it also has some limitations. Accordingly, a novel centralized droop-based control strategy considering N-1 contingency is proposed in this paper. It prevents converters from exceeding their limits while causes optimal power sharing and minimum DC link voltage deviation immediately, without secondary control layer. It also utilizes maximum wind power without curtailment. These properties improve the performance of the MTDC system in post-contingency conditions. The effectiveness of the proposed control method is validated by simulation of a 4-terminal VSC-MTDC system in MATLAB/Simulink R2016a.

Keywords: DC Voltage Control, Droop-Based Control, Optimal Power Sharing, Post-Contingency Conditions, VSC-MTDC System.

1 Introduction

In recent years, advances in semiconductor technologies, voltage source converters (VSCs), current source converters (CSCs), and DC circuit breakers have led to the development of point-to-point HVDC systems toward multi-terminal HVDC (MTDC) systems [1]. Nowadays, VSC-MTDC systems are more desirable due to their advantages, such as independent control of active (P) and reactive power (Q) and reversing the direction of power transmission without changing the DC voltage polarity [2-4].

Power sharing and DC voltage control in post-contingency conditions are the main challenges of MTDC systems [5]. The control structure of MTDC systems is divided into "low level" (including inner current and firing control of the VSCs) and "high level" (including primary and secondary control layer) [6]. The primary control layer is responsible for power sharing and DC voltage control immediately after disturbances occur [7]. The secondary control layer adjusts the optimal references of converters based on various purposes (e. g., minimizing losses) [8]. The three main control methods of the primary control layer are the master-slave, voltage margin, and droop method [9]. The master-slave method has disadvantages such as low reliability and the need for a high-rating master converter [10, 11]. The voltage margin method is an extension of the master-slave that, despite increasing reliability, suffers from complication and high stress on converters [12-14]. The droop method was introduced based on the concept of frequency regulation in AC systems. In this method, all converters participate in the control of DC link voltage, which increases reliability. Therefore, it is a more appropriate choice than the other two methods. More details and various development of droop control methods are presented in [15-19].

Using fixed droop coefficients without considering the

Iranian Journal of Electrical and Electronic Engineering, 2022.
Paper first received 22 February 2021, revised 02 August 2021, and accepted 13 August 2021.
* The authors are with the Department of Electrical Engineering, Ferdowsi University of Mashhad, Mashhad, Iran.
E-mails: s.m.alavi@mail.um.ac.ir and rghazi@um.ac.ir.
Corresponding Author: R. Ghazi.
https://doi.org/10.22068/IJEEE.18.1.2114

actual loading conditions causes the converters to exceed their limits in the post-contingency conditions. Also, employing local voltage feedback prevents accurate power sharing due to the DC line resistance and its effect on the DC voltage deviation. To overcome these drawbacks, adaptive droop-based control has been introduced. In [20], the adaptive droop coefficients are proposed based on the available headroom of converters. However, the DC link voltage and optimal power sharing are not considered. In [21], droop coefficients are suggested as a variable resistor based on the line resistance to minimize losses in post-contingency conditions. In [22], adaptive droop control is proposed using fuzzy logic and tradeoff between power sharing and DC voltage deviation. Reference [23] introduces adaptive droop coefficients based on voltage and power deviation indices to prevent the converters from exceeding their limit in post-contingency conditions. However, optimal power sharing does not occur. In [24], the adaptive droop control is implemented in both AC grid-side and wind farms converters to regulate the DC voltage within the desired level and prevent the converters from exceeding their limits in post-contingency conditions. Reference [25] proposes adaptive droop coefficients based on trajectory sensitivity analysis and stability constraints so that converters do not exceed their limits under the converter outage. In [26], an adaptive droop control strategy is proposed to achieve a faster dynamic response of MTDC systems. It prevents the output power and voltage from exceeding their limits without considering the optimal power sharing. In [27] a modified adaptive droop control is presented based on the converters' available headroom (AH) and loading factor (LF) to minimize the power sharing burden on converters during power variations/consecutive disturbances while maintaining the constraints of the DC grid without optimal operation.

A detailed linearized model of the system dynamics (such as AC grid, DC grid, AC connection filters, and inner controllers) and OPF approach in the secondary control layer are proposed in [28] and [29] to design droop control and obtain optimal power sharing, respectively. These two methods are not suitable for large systems due to their complicated calculations. Reference [30] introduces a power sharing index among neighboring converters to improve the stability during the latencies in communication signals and achieve accurate power sharing regardless of MTDC structure and DC line resistance. Although, the DC link voltage is ignored. Reference [31] proposes a developed droop control to improve the stability of the MTDC grid. It only considers the converter outage while ignoring other contingencies and optimal power sharing. In [32], droop coefficients are proposed so that the DC voltage (both transient and steady-state) and active power of converters do not exceed their limit under disturbances. Reference [33] proposes a coordinated droop controller based on Model Predictive Control (MPC) to minimize the DC voltages deviations of the MTDC system and avoid control mode change of droop VSCs in severe conditions. In [34], describes a control strategy consisting of a linear quadratic controller and an adaptive droop method is introduced to maintain stability in post-contingency conditions. Reference [35] proposes a methodology based on the concept of over- and under-voltage containment reserves for determining droop coefficients to guarantee the voltage security in MTDC grid.

The time interval between disturbance detection and implementation of the secondary control layer can cause destructive effects on the neighboring AC grid (e.g., frequency deviation) and stability that has not been considered in the previous works. Maintain optimal operation of MTDC system in post-contingency condition immediately after disturbance detection, overcome these drawbacks. Accordingly, in this paper, a centralized droop-based control strategy in the presence of high bandwidth communication is proposed. In this method, the central controller determines the optimal droop coefficients based on the prediction of N-1 contingency (change in output power of WFs, converter outage, and DC line disconnection) and stored them. Then, it applies the predetermined optimal droop coefficients to the converters immediately at the first control layer after disturbance detection in post contingency conditions. In addition to optimal power sharing, the proposed optimal droop coefficients maintain DC voltage and active power of VSC stations within their limit. They also minimize DC link voltage deviation and cause maximum utilization from the output power of WFs without any curtailment. Furthermore, the proposed approach includes stability constraints to consider the droop effect on the stable operation of the MTDC system.

The rest of this paper is organized as follows: Section 2 introduces the VSC-MTDC system model and its control structure. Section 3 describes the proposed droop-based control strategy. Simulations of a 4-terminals VSC-MTDC system are carried out on MATLAB/Simulink to validate the proposed control strategy in Section 4. The conclusion is shown in Section 5.

2 Modeling of VSC-MTDC

Fig. 1 shows the VSC-MTDC system schematic and the control structure of the VSCs used in it. The AC grid is modeled as a voltage source (V_s) and Thevenin impedance (R_S + jX_S). It is connected to the VSC by an AC transformer, high-pass filter, and a phase reactor.

The inner current control loop can be implemented by direct or vector control. The separate control capability of active and reactive power based on the park's transformation makes the vector method a more appropriate choice. It uses the dynamic equations of the

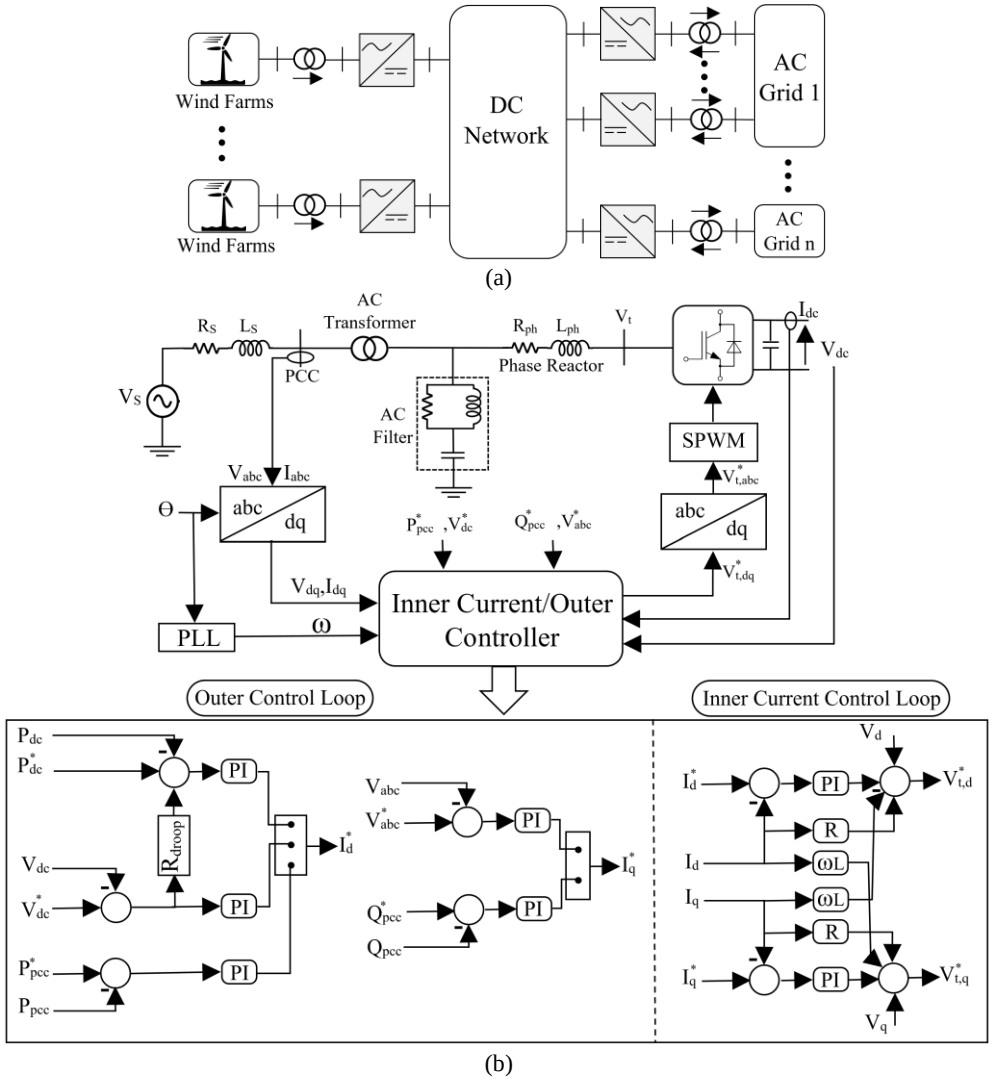

Fig. 1 a) VSC-MTDC configuration and b) Control structure of the VSC station.

system, which are expressed by [5]:

$$\begin{bmatrix} V_{t,d} \\ V_{t,q} \end{bmatrix} - \begin{bmatrix} V_d \\ V_d \end{bmatrix} = R \begin{bmatrix} I_d \\ I_q \end{bmatrix} + L \frac{d}{dt} \begin{bmatrix} I_d \\ I_q \end{bmatrix} + \omega L \begin{bmatrix} 0 & -1 \\ 1 & 0 \end{bmatrix} \begin{bmatrix} I_d \\ I_q \end{bmatrix} \quad (1)$$

R and L refer to equivalent resistance and inductance of the AC transformer, AC filter, and phase reactor. The inner current control loop uses a PI controller, although some references such as [36] and [37] have used sliding mode control (SMC). The reference values I_d^* and I_q^* used in the inner current control loop are determined by the outer control loop. I_q^* and I_d^* are determined by reactive power and AC voltage, and active power and DC voltage based on the constant-voltage, constant-power, and droop mode.

3 The Proposed Droop-based Control Strategy

Power sharing and DC link voltage control are the principal duties of the droop control method in post-contingency conditions. Droop control is implemented based on power (P-V curve) used in this paper or current (I-V curve [38]). Also, common voltage feedback and communication structure are used to eliminate the impact of DC line resistance and system configuration on accurate power sharing such as [39]. Fig. 2 shows the P-V characteristic curve and implementation of the proposed control strategy.

The central controller detects disturbances by online monitoring of power (P_i) and voltage (V_i) at the DC buses. Then it applies the optimal droop coefficients to the converters. In many communication-based MTDC controllers, time delays are considered in the order of 1-10 ms that has no significant effect on system stability [40]. To decrease the latencies, the central controller use from real-time data transmission in the platform of a high bandwidth communication system. Droop coefficient (R_{droop}) indicates the relation between power and voltage of each converter, which is related to the slope of the P-V characteristic curve by [9]:

$$R_{droop} = \frac{P_n}{V_n \beta_{droop}} \quad (2)$$

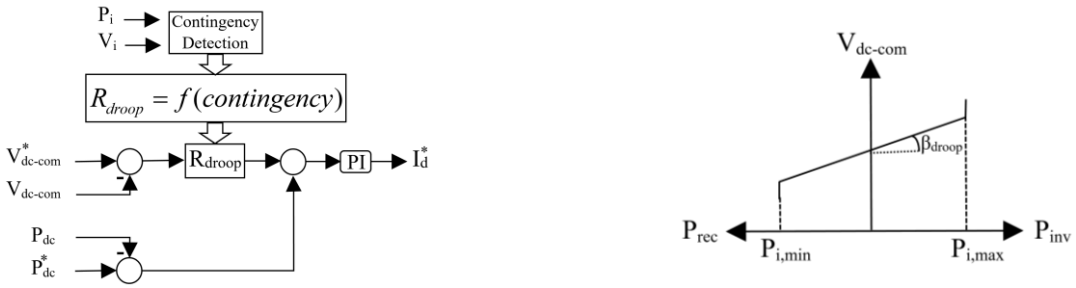

(a) (b)

Fig. 2 a) The proposed droop control schematic and b) (P-V) droop characteristic curve.

where P_n and V_n are the rated power and voltage, respectively. Increasing droop coefficients to reduce DC link voltage deviation threatens the stability. Therefore, they are limited by droop constraints. The maximum Droop coefficients are obtained by modal analysis of differential-algebraic equations (DAEs) of the system [5, 41]. Optimal droop coefficients are predicted before the occurrence of disturbance and used immediately after contingency detection. Therefore, the secondary control layer is not required. These coefficients are updated based on new operating conditions to be used in the next contingency. They cause the power sharing ratio to have the least deviation from the initial optimal conditions for minimizing the disturbance impact on neighboring AC systems. It is assumed that converters '1:*m*' and '*m*+1:*n*' operate in droop and constant-power mode, respectively. Determining the optimal droop coefficients based on various contingencies is discussed as follows.

3.1 Change in Output Power of WFs

The constrained nonlinear optimization problem to determine the optimal droop coefficients during the change in output power of *j*-th wind farm is expressed by

$$\max \quad P^* \qquad s.t \begin{cases} V_{i,\min} \le V_i \le V_{i,\max} & i = 1:n \\ P_i \le P_{i,\max} & i = 1:m \\ P_i = P_{i,0} - \alpha R_i \Delta V_1 & i = 1:m \\ P_i = P_{i,0} & i = m+1:n; i \ne j \\ P_i = P^* & i \ne j \\ R_i = R_{i,0} & i = 1:m; i \ne k_1,...,k_j \\ 0 \le \alpha R_i \le R_{i,\max} & i = k_1,...,k_j \end{cases} \tag{3}$$

where P_i and V_i are the active power and DC voltage at VSC stations, respectively. P_i is determined based on power flow equations by

$$P = V \odot (YV) \tag{4}$$

where V and Y refer to the DC voltage vector and admittance matrix of the DC grid, respectively. The symbol $\odot$ is the Hadamard product operator. To find the droop coefficients based on the output power of WFs, optimization problem (4) is solved in several steps. First, the maximum wind power is obtained according to the initial droop coefficients ($k_i = 0$). In the next step, the droop coefficient, which its associated power constraint is activated in the previous step, is allowed to change. If any of the voltage constraints are activated, the droop coefficient, which minimizes (5), is allowed to change ($i = k_1$), too. Then optimization problem (4) with modified constraints is solved.

$$\min \left\{ (R_{i,\max} - R_{i,0}) \left(R_{\max,0} / R_{i,0} \right) \right\} \tag{5}$$

This process continues to achieve the optimal droop coefficients according to the maximum output power of WFs at each step while the converters remain within their limits. To more accurately estimate the droop coefficients during the change of wind power in each step, the optimization problem is expressed as

$$for \quad l = 1:N \begin{cases} \min \quad \sum_{\substack{i=1 \\ i \ne j}}^{m} \left(\frac{R_i - R_{i,0}}{R_{i,0}} \right)^2 \\ s.t \begin{cases} V_{i,\min} \le V_i \le V_{i,\max} & i = 1:n \\ P_i \le P_{i,\max} & i = 1:m \\ P_i = P_{i,0} - \alpha R_i \Delta V_1 & i = 1:m \\ P_i = P_{i,0} & i = m+1:n; i \ne j \\ P_i = P^*_{spec,l} & i = j \\ R_i = R_{i,0} & i = 1:m; i \ne k_1,...,k_j \\ 0 \le \alpha R_i \le R_{i,\max} & i = k_1,...,k_j \end{cases} \end{cases} \tag{6}$$

Problem (6), according to the desired accuracy (N), determines the optimal droop coefficients related to several specific powers in each step ($P^*_{spec,l}$). Finally, the function of droop coefficients according to wind power changes is obtained by interpolation.

3.2 Converter Outage

The constrained nonlinear optimization problem with considering outage of the *j*-th converter is determined by

$$\min \quad \sum_{\substack{i=1 \\ i\neq j}}^{m}\left(\frac{R_i - R_{i,0}}{R_{i,0}}\right)^2$$

$$s.t\begin{cases} V_{i,\min} \le V_i \le V_{i,\max} & i=1:n; i\neq j \\ P_i \le P_{i,\max} & i=1:m; i\neq j \\ P_i = P_{i,0} - \alpha R_i \Delta V_1 & i=1:m; i\neq j \\ P_i = 0 & i=j \\ P_i = P_{i,0} & i=m+1:n \\ R_i = R_{i,0} & i=k_1,...,k_j; i\neq j \\ 0 \le \alpha R_i \le R_{i,\max} & i=1:m; i\neq k_1,...,k_j \end{cases} \quad (7)$$

where P_i is determined by (4). The process of determining the optimal droop coefficients is as follows. First, the problem is solved by assuming that all droop coefficients are allowed to change. Then, if the power constraints are activated, their associated droop coefficients are still allowed to change. If any voltage constraint is activated, the droop coefficient with the lowest index expressed by (5) is also allowed to change. The other droop coefficients are considered equal to their initial value, and optimization problem (7) is modified with the revised constraints. If it does not have an optimal solution, the second droop coefficient with the lowest index expressed by (5) is also allowed to change. Then, problem (7) is modified again with the new constraints. This process continues until the optimal coefficients are determined.

The outage of the first converter causes inappropriate operation of the system because it depends on (ΔV_1). Accordingly, optimization problem (7) must be defined based on another voltage feedback (e.g., ΔV_2) to increase reliability.

3.3 DC Line Disconnection

The constrained nonlinear optimization problem with considering disconnection of any DC line is expressed by

$$\min \quad \sum_{i=1}^{m}\left(\frac{R_i - R_{i,0}}{R_{i,0}}\right)^2$$

$$s.t\begin{cases} V_{i,\min} \le V_i \le V_{i,\max} & i=1:n \\ P_i \le P_{i,\max} & i=1:m \\ P_i = P_{i,0} - \alpha R_i \Delta V_1 & i=1:m \\ P_i = P_{i,0} & i=m+1:n \\ R_i = R_{i,0} & i=1:m; i\neq k_1,...,k_j \\ 0 \le \alpha R_i \le R_{i,\max} & i=k_1,...,k_j \end{cases} \quad (8)$$

where P_i is determined by modifying (4) while considering the impact of DC line disconnection on the admittance matrix. First, assuming that all droop coefficients are allowed to change ($k_i \neq 0$), optimization problem (8) is solved. Then, the proposed process in Subsection 3.2 is applied to achieve optimal droop coefficients. If any converter is isolated from the MTDC system by DC line disconnection, its power and voltage constraints are not considered.

4 Simulation Results

Fig. 3 shows the configuration of a (±320 kV) bipolar 4-terminal VSC-MTDC system simulated in MATLAB/Simulink R2016a. It consists of one wind farm (with AC voltage and frequency control mode) and three AC grids (with Droop control mode). The rectifier and the inverters are three-level Neutral Point Clamped (NPC) VSC converters using close IGBT/Diodes. They utilize the sinusoidal pulse width modulation (SPWM) technique. The VSC station includes on the AC side: The Yg-D transformer, the AC filters, the converter reactor, and on the DC side: the capacitors, the DC filter.

The line distance, rated power (P_n), and slope (β_{droop}) of VSCs are shown in Fig. 3. The central controller uses a high-bandwidth communication system for online monitoring of the MTDC system. It calculates the optimal droop coefficients and immediately applies them to the VSCs in the post-contingency conditions. The SQP algorithm is one of the most powerful algorithms in solving large-scale nonlinear optimization problems [42]. It is utilized to solve proposed optimization problems. The parameters of the VSC-MTDC test system are given in Table 1.

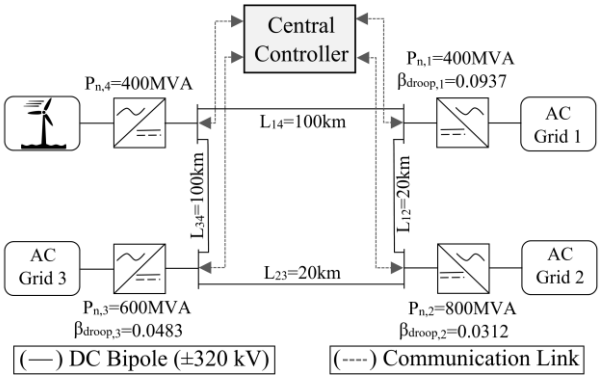

Fig. 3 Configuration of 4-terminal VSC-MTDC test system.

Table 1 The VSC-MTDC test system parameters.

Line voltage of AC grid (rms)	370 kV
Equivalent resistance of AC system	0.08 Ω
Equivalent inductance of AC system	0.025 H
Fundamental frequency	50 Hz
Carrier frequency as multiple of fundamental	27 Hz
Limit of the DC voltage deviation	25 kV
The phase reactor	0.15 pu
Transformer	2000 MVA, 370/320 kV, YgD,0.15 pu
Unit resistance of the DC line	0.4 Ω/km
Unit inductance of the DC line	0.45 mH/km
Unit capacitance of the DC line	23 μF/km
Rated DC voltage	±320 kV
K_I of outer/inner control loop	6
K_P of inner control loop	0.6

Table 2 Initial optimal steady-state operating point of VSC-MTDC system.

Terminal No.	VSC_1	VSC_2	VSC_3	VSC_4
Power [MW]	100	600	291.1	1000
DC voltage [kV]	640	639.23	640.34	645.39

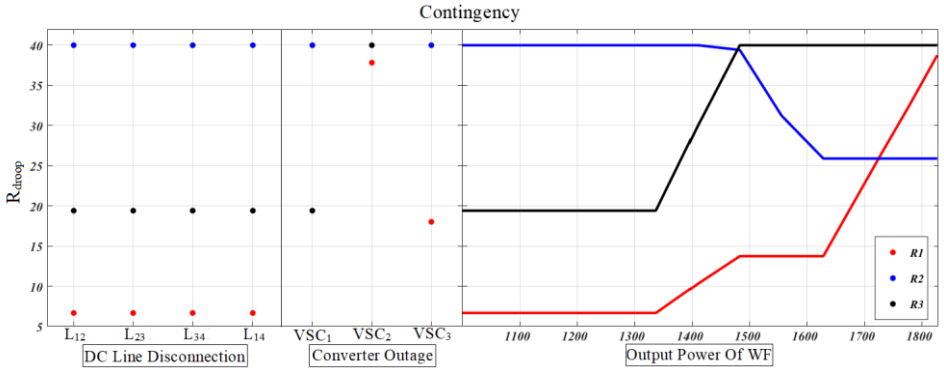

Fig. 4 The optimal droop coefficients under various contingencies in the initial operating conditions.

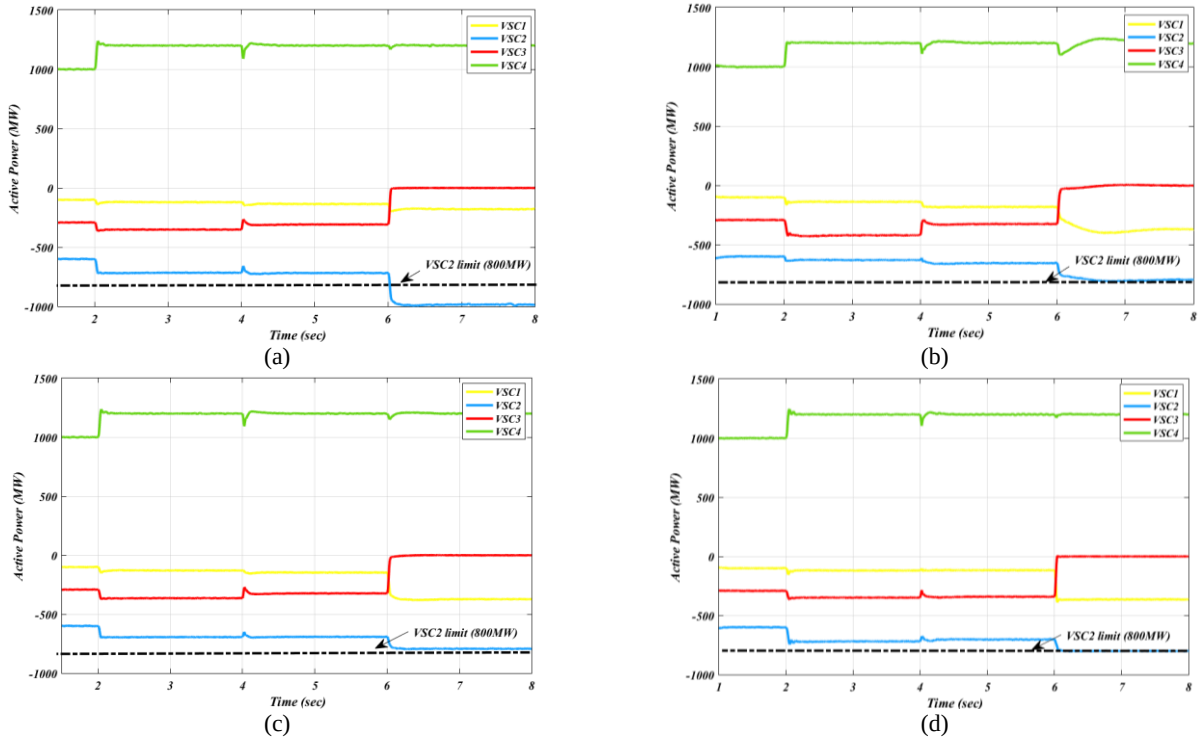

Fig. 5 Active power at VSC stations in: a) fixed droop control, b) adaptive P-based droop control [20], c) adaptive P-V-based droop control [23], and d) proposed droop control.

The initial optimal steady-state operating point of the VSC-MTDC system is shown in Table 2.

Fig. 4 demonstrates the predicted optimal droop coefficients under different contingencies. It is obtained based on the initial conditions mentioned in Table 2, which is updated by changing the operating conditions.

The proposed method is compared with the fixed droop control, adaptive droop control based on available headroom of VSCs [20], and adaptive droop control based on a tradeoff between power and voltage of VSCs [23] to validate its superiority. They are applying to the MTDC system during the following disturbances:

1. In t = 2 sec, an increase of the wind power by 200 MW.
2. In t = 4 sec, disconnection of L_{34}.
3. In t = 6 sec, disconnection of VSC_3.

The initial optimal power sharing ratio between VSC_1, VSC_2, and VSC_3 is 1, 6, and 2.91, respectively, which should be retained as much as possible. Fig. 5 illustrates the power sharing between grid converters during various contingencies by the mentioned methods. Fig. 5(a) shows that sharing the wind power between VSC_1, VSC_2, and VSC_3 is not proportional to their droop coefficients (1, 6, and 2.91) due to local voltage feedback (e.g., deviation from desired values in VSC_1, VSC_2, and VSC_3 is "+0.41%, -0.42%, and +0.72%", and "+15.87%, +2.11%, and –9.67%" during first and second disturbances, respectively). Furthermore, it

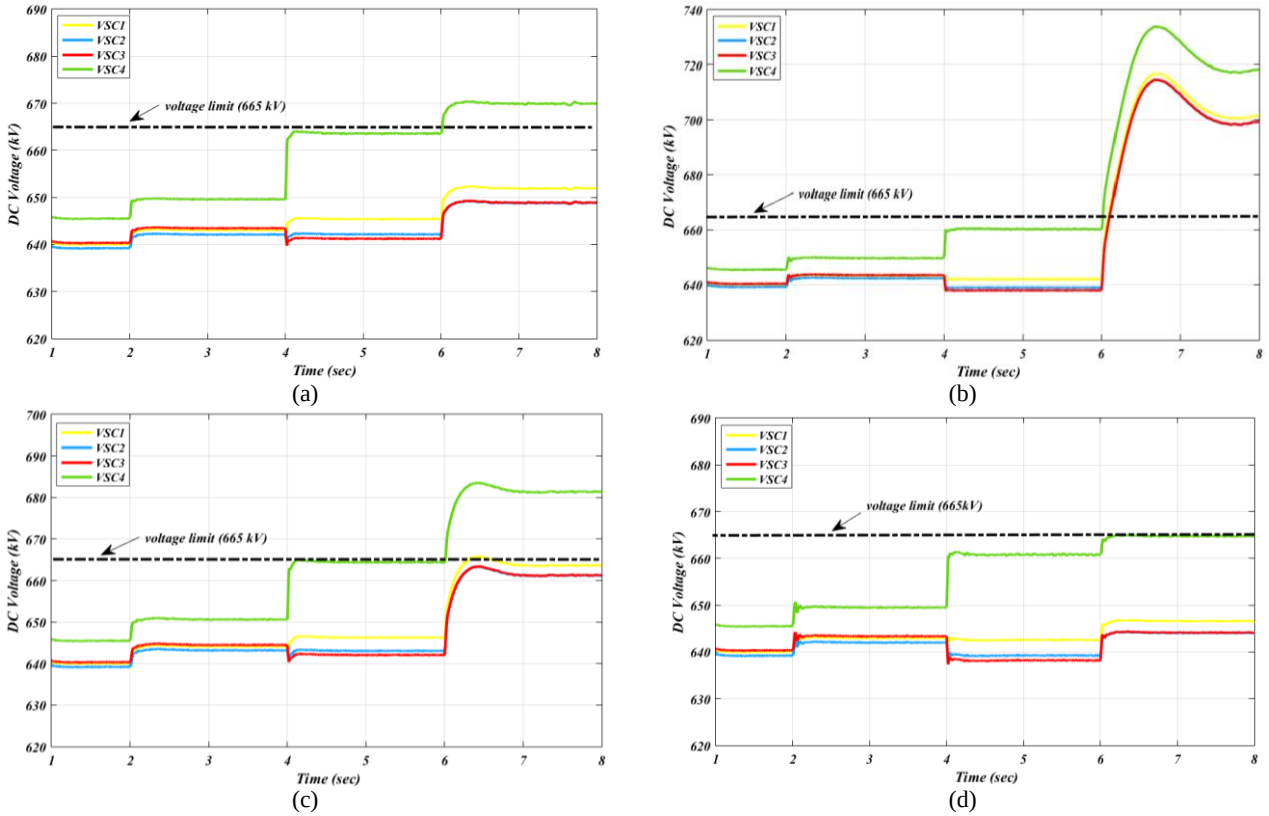

Fig. 6 DC voltage at VSC stations: a) fixed droop control, b) adaptive P-based droop control [20], c) adaptive P-V-based droop control [23], and d) proposed droop control.

shows that active power at the VSC_2 station is 23% more than its rating under the third contingency. Fig. 5(b) shows that although the converters do not exceed their rating, optimal power sharing does not occur. Fig. 5(c) also shows similar results. However, it has more reasonable power sharing. For instance, the power sharing ratio between VSC_1, VSC_2, and VSC_3 change from "1, 0.76, and 3.38" to "1, 3.18, and 2.47" during the first disturbance. It means that active power deviation from desired values in VSC_1, VSC_2, and VSC_3 change from "+15.35%, -12.49%, and +20.56%" to "+8.1%, -3.46%, and +4.38%". Fig. 5(d) indicates that the converters remain within their rating while optimal power sharing has also occurred (e.g., the power sharing ratio between VSC_1, VSC_2, and VSC_3 is "1, 6, and 2.91" during first and second disturbances). During the third contingency, VSC_2 operates at its rated power (800 MW) due to its limitation.

Fig. 6 illustrates the DC voltage variation at VSC stations in post-contingency conditions. Fig. 6(a) indicates that DC voltage at the VSC_4 station exceeds the allowable limit by 0.72% (4.79 kV) during the 3rd disturbance. Fig. 6(b) shows that DC voltage at VSC_1, VSC_2, and VSC_4 stations exceeds the permissible limit by 5.7%, 5.36%, and 8.21%, respectively, under the 3rd disturbance. It occurs due to ignoring the voltage impact on the determination of droop coefficients. Fig. 6(c) shows that DC voltage at the VSC_4 station exceeds the allowable limit by 2.45% (16.31 kV) during the 3rd disturbance. The DC voltage of other converters due to considering voltage impact on droop coefficients remains within their limit in post-contingency conditions. Fig. 6(d) indicates that deviation from rated DC voltage is less than other methods, and all converters do not exceed their limits.

The DC voltage deviation at the VSC_4 station during the third contingency has increased 19.16%, 178.5%, and 65.2% more than acceptable voltage deviation margin (25 kV) in fixed droop, adaptive P-based droop, and adaptive P-V-based droop methods, respectively. Furthermore, the maximum DC link voltage deviation at VSCs with droop mode control is 79.5% (fixed droop), 549.6% (adaptive P-based droop), and 258.2% (adaptive P-V-based droop) more than the proposed method (6.61 kV). It has occurred in VSC1 during third contingency.

5 Conclusion

In this paper, a centralized droop-based control strategy based on predicting N-1 contingency is proposed. Various contingencies such as changing the output power of WFs, disconnection of DC line, and converter outage are studied. The proposed control strategy guarantees optimal power sharing and minimum DC link voltage deviation in post-contingency conditions immediately. It improves stability and reduces the destructive effect of disturbances on the

neighboring AC system by eliminating the secondary control layer. Also, active power and DC voltage at VSC stations remain within their limits. The proposed method is compared with fixed, adaptive P-based, and adaptive P-V-based droop methods under various contingencies in MATLAB/Simulink environment. Simulation results demonstrate the effectiveness and superiority of the proposed control strategy in post-contingency conditions.

Intellectual Property

The authors confirm that they have given due consideration to the protection of intellectual property associated with this work and that there are no impediments to publication, including the timing of publication, with respect to intellectual property.

Funding

No funding was received for this work.

CRediT Authorship Contribution Statement

S. M. Alavi: Conceptualization, Methodology, Software, Formal analysis, Writing - Original draft. **R. Ghazi:** Supervision, Revise & editing.

Declaration of Competing Interest

The authors hereby confirm that the submitted manuscript is an original work and has not been published so far, is not under consideration for publication by any other journal and will not be submitted to any other journal until the decision will be made by this journal. All authors have approved the manuscript and agree with its submission to "Iranian Journal of Electrical and Electronic Engineering".

References

[1] P. Rodriguez and K. Rouzbehi, "Multi-terminal DC grids: challenges and prospects," *Journal of Modern Power System and Clean Energy*, Vol. 5, No. 4, pp. 512–523, Jul. 2017.

[2] S. Cole, J. Beerten, and R. Belmans, "Generalized dynamic VSC MTDC model for power system stability studies," *IEEE Transaction on Power System*, Vol. 25, No. 3, pp. 1655–1662, Aug. 2010.

[3] A. Korompili, Q. Wu, and H. Zhao, "Review of VSC HVDC connection for offshore wind power integration," *Renewable and Sustainable Energy Reviews*, Vol. 59, pp. 1405–1414, Jun. 2016.

[4] N. Flourentzou, V. G. Agelidis, and G. D. Demetriades, "VSC-based HVDC power transmission systems: An overview," *IEEE Transactions on Power Electronic*s, Vol. 24, No. 3, pp. 592–602, Mar. 2009.

[5] N. Chaudhuri, B. Chaudhuri, R. Majumder, and A. Yazdani, *Multi-terminal direct-current grids: Modeling, analysis, and control*. New Jersey, Wiley-IEEE Press, 2014.

[6] F. D. Bianchi, J. L. D. García, and O. G. Bellmunt, "Control of multi-terminal HVDC networks towards wind power integration: A review," *Renewable and Sustainable Energy Review*, Vol. 55, pp. 1055–1068, Mar. 2016.

[7] F. Akhter, "Secure optimal operation and control of integrated AC/MTDC meshed grids," *Ph.D. Thesis*, University of Edinburgh, Scotland, 2015.

[8] M. A. Peñalba, A. E. Àlvarez, S. G. Arellano, and O. G. Bellmunt, "Droop control for loss minimization in HVDC multi-terminal transmission systems for large offshore wind farms," *Electric Power Systems Research*, Vol. 112, pp. 48–55, Jul. 2014.

[9] J. Beerten, "Modeling and control of DC grids," *Ph.D. Thesis*, Arenberg Doctoral School, Belgium, 2013.

[10] J. Cao, W. Du, H. F. Wang, and S. Q. Bu, "Minimization of transmission loss in meshed AC/DC grids with VSC-MTDC networks," *IEEE Transaction on Power Systems*, Vol. 28, No. 3, pp. 3047–3055, Aug. 2013.

[11] L. Xu and L. Yao, "DC voltage control and power dispatch of a multi-terminal HVDC system for integrating large offshore wind farms," *IET Renewable Power Generation*, Vol. 5, No. 3, pp. 223–233, Jun. 2011.

[12] T. Nakajima and S. Irokawa, "A control system for HVDC transmission by voltage sourced converters," in *IEEE Power Engineering Society Summer Meeting*, Edmonton, Canada, 1999.

[13] C. Dierckxsens, K. Srivastava, M. Reza, S. Cole, J. Beerten, and R. Belmans, "A distributed dc voltage control method for VSC-MTDC systems," *Electric Power Systems Research*, Vol. 82, No. 1, pp. 54–58, Jan. 2012.

[14] J. Beerten, S. Cole, and R. Belmans, "Modeling of multi-terminal VSC HVDC systems with distributed DC voltage control," *IEEE Transactions on Power Systems*, Vol. 29, No. 1, pp. 34–42, Jan. 2013.

[15] B. Berggren, K. Lindén, and R. Majumder, "DC grid control through the pilot voltage droop concept methodology for establishing droop constants," *IEEE Transaction on Power System*, Vol. 30, No. 5, pp. 2312–2320, Sep. 2015.

[16] Y. Wang, B. Li, Z. Zhou, Zh. Chen, W. Wen, X. Li, and Ch. Wang, "DC voltage deviation-dependent voltage droop control method for VSC-MTDC systems under large disturbances," *IET Renewable Power Generation*, Vol. 14, No. 5, pp.891–896, Mar. 2020.

[17] J. Beerten and R. Belmans, "Analysis of power sharing and voltage deviations in droop-controlled dc grids," *IEEE Transaction Power System*, Vol. 28, No. 4, pp. 4588–4597, Nov. 2013.

[18] Y. Gao and Q. Ai, "Distributed multi-agent control for combined AC/DC grids with wind power plant clusters," *IET Generation, Transmission & Distribution*, Vol. 12, No. 3, pp. 670–677, Feb. 2018.

[19] G. Stamatiou and M. Bongiorno, "Power-dependent droop-based control strategy for multi-terminal HVDC transmission grids," *IET Renewable Power Generation*, Vol. 11, No. 2, pp. 383–391, Jan. 2017.

[20] N. R. Chaudhuri and B. Chaudhuri, "Adaptive droop control for effective power sharing in multi-terminal DC (MTDC) grids," *IEEE Transaction Power System*, Vol. 28, No. 1, pp. 21–29, Feb. 2013.

[21] A. S. Abdel-Khalik, A. M. Massoud, A. A. Elserougi, and Sh. Ahmed, "Optimum power transmission-based droop control design for multi-Terminal HVDC of offshore wind farms," *IEEE Transactions on Power Systems*, Vol. 28, No. 3, pp. 3401–3409, Aug. 2013.

[22] X. Chen, L. Wang, H. Sun, and Y. Chen, "Fuzzy logic based adaptive droop control in multi-terminal HVDC for wind power integration," *IEEE Transactions on Energy Conversion*, Vol. 32, No. 3, pp. 1200–1208, Sep. 2017

[23] Y. Wang, W. Wen, Ch. Wang, H. Liu, X. Zhan, and X. Xiao, "Adaptive voltage droop method of multi-terminal VSC-HVDC systems for DC voltage deviation and power sharing," *IEEE Transaction Power Delivery*, Vol. 34, No. 1, pp. 169–176, Feb. 2019.

[24] A. S. Kumar and B. P. Padhy, "Adaptive droop control strategy for autonomous power sharing and DC voltage control in wind farm-MTDC grids," *IET Renewable Power Generation*, Vol. 13, No. 16, pp. 3180–3190, Dec. 2019.

[25] A. Yogarathinam and N. R. Chaudhuri, "Stability-constrained adaptive droop for power sharing in AC-MTDC grids," *IEEE Transactions on Power Systems*, Vol. 34, No. 3, pp. 1955–1965, May 2019.

[26] M. Mei, P. Wang, Y. Che, and Ch. Xing, "Adaptive coordinated control strategy for multi-terminal flexible DC transmission systems with deviation control," *Journal of Power Electronics*, Vol. 21, No. 4, pp. 724–734, Feb. 2021.

[27] S. S. Sayed and A. M. Massoud, "A generalized approach for design of contingency versatile DC voltage droop control in multi-terminal HVDC networks," *International Journal of Electrical Power & Energy Systems*, Vol. 126, p. 106413, Mar. 2021.

[28] E. Prieto-Araujo, A. E. Alvarez, S. Fekriasl, and O. G. Bellmunt, "DC voltage droop control design for multi-terminal HVDC systems considering AC and DC grid dynamics," *IEEE Transaction on Power Delivery*, Vol. 31, No. 2, pp. 575–585, Apr. 2016.

[29] M. A. Abdelwahed and E. F. El-Saadany, "Power sharing control strategy of multi-terminal VSC-HVDC transmission systems utilizing adaptive voltage droop," *IEEE Transactions on Sustainable Energy*, Vol. 8, No. 2, pp. 605–615, Apr. 2017.

[30] A. Kirakosyan, E. F. El-Saadany, M. S. El Moursi, S. Acharya, and K. Al Hosani, "Control approach for the multi-terminal HVDC system for the accurate power sharing," *IEEE Transaction Power System*, Vol. 33, No. 4, pp. 4323–4334, Jul. 2018.

[31] M. Belgacem, M. Khatir, M. A. Djehaf, S. A. Zidi, and R. Bouddou, "Implementation of DC voltage controllers on enhancing the stability of multi-terminal DC grids," *International Journal of Electrical and Computer Engineering (IJECE)*, Vol. 11, No. 3, pp. 1894–1904, Jun. 2021.

[32] B. Li, Q. Li, Y. Wang, W. Wen, B. Li, and L. Xu, "A novel method to determine droop coefficients of DC voltage control for VSC-MTDC system," *IEEE Transactions on Power Delivery*, Vol. 35, No. 5, Oct. 2020.

[33] G. Li, Z. Du, C. Shen, Z. Yuan, and G. Wu, "Coordinated design of droop control in MTDC grid based on model predictive control," *IEEE Transactions on Power Systems*, Vol. 33, No. 3, pp. 2816–2828, May 2018.

[34] O. Yadav, Sh. Prasad, N. Kishor, R. Negi, and Sh. Purwar, "Controller design for MTDC grid to enhance power sharing and stability," *IET Generation, Transmission & Distribution*, Vol. 14, No. 12, Mar. 2020.

[35] K. Shinoda, A. Benchaib, J. Dai, and X. Guillaud, "Over- and under-voltage containment reserves for droop-based primary voltage control of MTDC grids," *IEEE Transactions on Power Delivery*, Jan. 2021.

[36] M. Nazari, "Control and planning of multi-terminal HVDC transmission systems," *Ph.D. dissertation*, KTH Royal Institute of Technology, Sweden, 2017.

[37] A. Moharana and P. K. Dash, "Input-output linearization and robust sliding-mode controller for the VSC-HVDC transmission link," *IEEE Transactions on Power Delivery*, Vol. 25, No. 3, pp. 1952–1961, Jul. 2010.

[38] O. G. Bellmunt, J. Liang, J. Ekanayake, and N. Jenkins, "Voltage-current characteristics of multi-terminal HVDC-VSC for offshore wind farms," *Electric Power Systems Research*, Vol. 81, No .2, pp. 440–450, Feb. 2011.

[39] A. Kirakosyan, E. F. El-Saadany, M. S. E. Moursi, and K. A. Hosani, "DC voltage regulation and frequency support in pilot voltage droop controlled multi terminal HVDC systems," *IEEE Transactions on Power Delivery*, Vol. 33, No. 3, pp. 1153–1164, Jun. 2018.

[40] I. M. Sanz, B. Chaudhuri, and G. Strbac, "Inertial response from offshore wind farms connected through dc grids," *IEEE Transactions on Power Systems*, Vol. 30, No. 3, pp. 1518–1527, May 2015.

[41] W. Wang, M. Barnes, and O. Marjanovic, "Stability limitation and analytical evaluation of voltage droop controllers for VSC MTDC," *CSEE Journal of Power and Energy Systems*, Vol. 4, No. 2, pp. 238–249, Jun. 2018.

[42] P. T. Boggs and J. W. Tolleb, "Sequential quadratic programming for large-scale nonlinear optimization," *Journal of Computational and Applied Mathematics*, Vol. 124, No. 1, pp.123-137, Dec. 2000.

S. M. Alavi (S'20) received the B.Sc. degree in Electrical Engineering from Iran University of Science and Technology (IUST), Tehran, Iran, in 2012 and the M.Sc. degree in Electrical Engineering from University of Tehran, Tehran, Iran, in 2015. He is currently pursuing the Ph.D. degree in Electrical Engineering at Ferdowsi University of Mashhad, Mashhad, Iran. His research interest includes power systems control and analysis, renewable energy generation, and multi-terminal HVDC transmission systems.

R. Ghazi (M'90) was born in Semnan, Iran in 1952. He received his B.Sc., degree (with honors) from Tehran University of Science and Technology, Tehran, Iran in 1976. In 1986 he received his M.Sc. degree from Manchester University, Institute of Science and Technology (UMIST), Manchester UK, and the Ph.D. degree in 1989 from the University of Salford UK, all in electrical engineering. Following the receipt of the Ph.D. degree, he joined the faculty of engineering at Ferdowsi University of Mashhad (FUM), Iran as an Assistant Professor of electrical engineering. He is now a Professor of Electrical Engineering in FUM, Iran. His main research interests are reactive power control, FACTS devices and custom power devices (CPD), application of power electronics in power systems, distributed generation (DG's), power quality. He has authored or coauthored more than 150 papers in these fields including four books.